


ARTICLE

Open Access



Nuclear magnetic resonance assignment strategy for pentacyclic triterpenes, using lup-20(29)-ene from *Pilotrichella flexilis* as model system, combining spectrally filtered proton-to-carbon schemes and DFT–GIAO approach

Jose Enrique Herbert-Pucheta^{1*} , Cinthia Mejía-Lara², Benito Reyes-Trejo², Lino Reyes³ and Holber Zuleta-Prada^{2*}

Abstract

The present work comprises a method to obtain full proton-to-carbon nuclear magnetic resonance chemical shift assignment of a C₃₀H₅₀ lup-20(29)-ene, for the first time obtained from the Mexican native mosses *Pilotrichella flexilis*, wherein said method consists in a combination of the following NMR schemes: 1D-¹³C (DEPT-135), 2D-{¹H–¹³C} HMBC with a spectral filter for promoting only weak-c.a. 2 Hz-long-range scalar couplings, 2D-{¹H–¹H} EXSY with long mixing times to favour only weak H–H dipolar correlations and ultra-high resolution one- and two-dimensional ¹H instant homodecoupling Psyche pure shift. Full set of assigned resonances were compared against the theoretical isotropic chemical shifts computed with a gauge invariant atomic orbital–density functional theory with self consistent reaction field calculation, retrieving accurate agreements, despite the intrinsic severe signal overlap that these C₃₀ hydrocarbon triterpenes experimentally present. Therefore, a 3D-structure supported by experimental NMR data of this type of important metabolite precursor in plants can be proposed.

Keywords: Pentacyclic triterpenes, NMR spectroscopy, Lupene, Weak long-range heteronuclear through-bound HMBC, Homonuclear proton long-range through-space EXSY, Pureshift NMR

Introduction

Triterpenoids belong to a very important and abundant class of naturally occurring compounds, with

approximately 20,000 structures identified to date [1–5]. In nature, triterpenes are often found as acyclic or mono-, di-, tri-, tetra- and penta-cyclic structures amongst others [6]. The interests in both pharmacological and biological activities of triterpenoids have continually increased in the last three decades [7]. The last is stressed by the constant increment of scientific reports demonstrating their biological and therapeutic potentials. Special attention to pentacyclic triterpenes (PTs) is evidenced, due to their biological broad-spectrum activities [8], such as anti-inflammatory, antioxidant, anti-viral, anti-diabetic, anti-tumoral, hepato-protective and cardio-protective effects [9–12]. Based on their

*Correspondence: jeherbert@conacyt.mx; hozuleta_13@comunidad.unam.mx

¹ Consejo Nacional de Ciencia y Tecnología – Laboratorio Nacional de Investigación y Servicio Agroalimentario y Forestal, Universidad Autónoma Chapingo, Km. 38.5 Carretera México-Texcoco, 56230 Chapingo, Estado de México, Mexico

² Laboratorio de Productos Naturales, Área de Química, Departamento de Preparatoria Agrícola, AP 74 Oficina de Correos Chapingo, Universidad Autónoma Chapingo, Km. 38.5 Carretera México-Texcoco, 56230 Chapingo, Estado de México, Mexico

Full list of author information is available at the end of the article

structural backbone and therapeutically properties, PTs can be classified within three major categories: *oleananes*, *ursanes* and *lupanes* types. Structural elucidation of both naturally or synthetic pentacyclic triterpenes, has been carried out mainly by means of liquid-state high-resolution NMR spectroscopy [13]. For complex PTs structural elucidation, combinations of one- and multi-dimensional NMR methods allow an attractive assignment strategy for hydrocarbon spin systems. However, despite enormous efforts in terms of finding accurate NMR multidimensional schemes for reaching complex assignments, complete proton/carbon NMR assignment of C₃₀ triterpenes with standard experiments could be cumbersome and unintuitive, mostly for those tetra- or penta-cyclic triterpenes lacking of multiple bonds or O-based, N-based, S-based, halogen-based, amongst others functional groups that conventional NMR assignment procedures use to anchor the connectivity pathways in complex spectra with intrinsic severe signal overlap in both proton and carbon chemical shift dimensions [14, 15]. Even when robust quantum chemistry calculations are carried out [16] to disentangle resonances in crowded regions within the experimental data, ambiguities can still be present, even with the use of costly computational schemes like post Hartree–Fock methods [17].

As part of our ongoing research to identify bioactive substances from native mosses [18], we have recently isolated and identified for the first time a pentacyclic triterpene lup-20(29)-ene coming from *Pilotrichella flexilis*, which is a common species broadly distributed along Mexico [19], and barely one phytochemical study of an oversea species has been reported until now [20]. Structures related to this type of PTs mainly comprised in higher plants, have also been observed in other ecosystems, including deep-sea fan, ancient sediments from high-moor peats as well as in several geological sources [21, 22].

Consequently, there is a need to propose a straightforward strategy for full unambiguous structure determination of PTs, possibly extended to general hydrocarbon aliphatic triterpenes in molecules present in natural product or geochemistry sciences. For that, the present study comprises a set of standard and recently proposed NMR experiments [23–26] for disentangling all spin systems—included proton shifts—of pentacyclic terpenoids.

Materials and methods

General experimental procedures

Melting points were determined with a Fisher-Johns apparatus without any further corrections. ¹H and ¹³C NMR spectra were performed on a Bruker 600 AVANCE III HD in CDCl₃ solution with tetramethylsilane (TMS) as internal standard (vide infra). Electronic Impact Mass

Spectrometry (EIMS) and High-Resolution Electrospray Ionization Mass Spectrometry (HRESIMS) were acquired respectively on a JEOL SX102A and a JEOL TheAccuTOF JMS-T100LC instruments. FT-IR spectroscopy was carried out in a Cary630 Agilent instrument. Silica gel 60 (Merck 70-230 Mesh ASTM) was used for column chromatography.

Plant material

The plant material was collected from locality “*La Mojonera*” (Municipality of Zacualtipán de Ángeles, Estado de Hidalgo, Mexico) on February 2017 and identified as *Pilotrichella Flexilis* by Mrs. Cinthía Mejía-Lara. A voucher was deposited in the herbarium (accession number 34591) of the Biology Facility of Departamento de Preparatoria Agrícola de la Universidad Autónoma Chapingo.

Extraction and isolation

Dried plant material (211 g) was extracted by triplicate with MeOH at room temperature. The methanolic extract was then evaporated at vacuum conditions, yielding a greenish residue, which was further suspended in H₂O and then extracted with *n*-hexane. Aqueous phase layer was further extracted with others solvents for additional studies out of the scope of the present work. Hexane extract (5.2 g) with full solvent removal, was chromatographed on a silica gel column with pentane and *n*-hexane as eluents. From the eluted fraction with pentane, lup-20(29)-ene was obtained with the following characteristics: white solid; Mp: 223 °C, IR (ATR, cm⁻¹) I_{max} 2919, 2851, 1458, 1240, 1035, 885; EIMS (70 eV) *m/z* 410 [M⁺] (20), 395 (17), 342 (8), 299 (9), 218 (8), 189 (100), 161 (19), 123 (29); HRESIMS *m/z* 411.39929 [M + H]⁺ (calculated for C₃₀H₅₁), Additional file 1: Figure S2.

Nuclear magnetic resonance spectroscopy

The following set of NMR experiments were conducted at a temperature of 298 K, stabilizing the temperature with a Bruker VCU flow unit:

- 1D-¹H 90° pulse direct excitation: A total of 64 transients were collected into 22 K complex data points, with a spectral width of 7812 Hz, recovery delay of 2 s and acquisition times of 1.4 s produces an experimental time of 6' 51". No apodization function was used prior to Fourier Transformation.
- 1D-¹H 90° real time instant homodecoupling pure shift: Homodecoupling was achieved with a Zangger–Sterk element comprising a Gaussian Refocusing Shaped pulse of 10 ms and a power level of 0.5 mW. A total of 2 K transients were collected into 9374 K

- complex data points, with a spectral width of 13 ppm (7812 Hz), recovery delay of 2 s and acquisition times of 600 ms produced an experimental time of 3 h 10' 56". No apodization function was used prior to Fourier Transformation.
- 1D- ^{13}C 90° pulse direct excitation: A total of 2048 transients were collected into 58 K complex data points, with a spectral width of 36,232 Hz and acquisition times of 800 ms with a recovery delay of 20 s per scan, produces an experimental time of 11 h 12' 6". Proton homonuclear broadband decoupling was carried out during ^{13}C signal acquisition, with a standard Waltz16 scheme. No apodization function was used prior to Fourier Transformation.
 - 1D- ^{13}C (DEPT): A DEPT polarization transfer scheme, with a $\{^1\text{H}\}$ -135 degree pulse at the middle of the final spin echo to produce CH/CH₃ positive signals and CH₂ negative signals was carried out with 4 K transients that were collected into 58 K complex data points, with a spectral width of 36,232 Hz and acquisition times of 800 ms with a recovery delay of 3 s per scan, produces an experimental time of 6 h 4' 25". Proton homonuclear broadband decoupling was carried out during ^{13}C signal acquisition, with a standard Waltz16 scheme. No apodization function was used prior to Fourier Transformation.
 - 2D- $\{^1\text{H}-^{13}\text{C}\}$ HMBC spectra were recorded by acquiring 7810 × 1024 points with 8 scans per transient. Heteronuclear $^1\text{H}-^{13}\text{C}$ spectral widths were setup respectively at 13,240 ppm. With acquisition times for the direct F2 dimension of 500 ms and a recovery delay of 2 s, both HMBC with different long-range evolution periods (τ) promoting only small (2 Hz, $\tau = 250$ ms, Fig. 3 and Additional file 1: Figure S5, top) and small to medium (7 Hz, $\tau = 62.5$ ms, Fig. 3 and Additional file 1: Figure S5, bottom) heteronuclear $^nJ_{\text{CH}}$ coupling constants, produced experimental times of respectively 6 h 6' 49" and 5 h 52' 34".
 - 2D- $\{^1\text{H}-^{13}\text{C}\}$ HSQC spectrum was recorded by acquiring 7810 × 1024 points with 8 scans per transient. Heteronuclear $^1\text{H}-^{13}\text{C}$ spectral widths were setup respectively at 13,180 ppm. An acquisition time for the direct F2 dimension of 500 ms and a recovery delay of 2 s produced an experimental time of 5 h 45' 44".
 - 2D- $\{^1\text{H}-^1\text{H}\}$ EXSY spectrum was carried out by acquiring 12498 × 512 points with 4 scans per transient. Spectral widths were setup in both dimensions at 13 ppm. An acquisition time of 800 ms (F2), a recovery delay of 3 s and a long mixing time of 1.4 s, produced an experimental time of 2 h 59' 37".
 - 2D- $\{^1\text{H}-^1\text{H}\}$ TOCSY-Pureshift Yielded by Chirp Excitation (PSYCHE) experiment was carried out as follows: The homonuclear Hartman–Hahn transfer was done with a DIPSI2 element during a mixing time of 500 ms, whilst the Chirp Excitation to achieve homonuclear decoupling was done with the Crp psyche adiabatic shaped pulse, comprising 30 ms pulse-length and a 0.22 mW power level. Experimental times of 4 h 19' 12" were recorded for experiments with 3124 × 512 complex points with 8 scans per F1 increment, spectral width of 13 ppm, acquisition times of 200 ms and a recovery delay of 3 s. A spectral symmetrisation procedure was carried out for a double Fourier Transformed spectrum with 8 K zero-filling points per F1/F2 dimension.
 - 2D- $\{^1\text{H}-^1\text{H}\}$ TOCSY spectrum was carried out by acquiring 12498 × 512 points with 8 scans per transient. Spectral widths were setup in both dimensions at 13 ppm. An acquisition time of 800 ms (F2), a recovery delay of 3 s and a DIPSI mixing time of 500 ms, produced an experimental time of 3 h 49' 55".

Computational methods

Geometry optimizations, electronic structure determinations and Nuclear Magnetic Resonance chemical shift tensors were computed using the program Gaussian 09 [27]. C₃₀H₅₀ lup-20(29)-ene geometry was optimized by an energy minimization procedure with respect all geometrical parameters, without imposing any molecular constraint. Restricted Hartree–Fock (RHF) was used as geometry pre-optimization scheme, taking as input the electronic structure of the Betulin-diacetate C₃₄H₅₄O₄ crystallographic data [28]. Density functional theory (DFT) procedure for energy minimization and orbital description was performed with the hybrid functional B3LYP [29, 30]. The standard 6-311G (2d,p) basis set was used for all H, C atoms. Harmonic vibrational frequency analysis of the most stable local minimum herein presented in Additional file 1: Figure S6 was carried out, with no observed imaginary frequencies. Gauge-Invariant Atomic Orbital (GIAO) scheme [31] was used to compute ^1H and ^{13}C chemical shift values, theoretically referenced to TMS/6-311G (d,p). Self-Consistent Reaction Field (SCRFF) Tomasi's Polarized Continuum (PCM) for solvation [32] was used in all calculations to describe implicitly chloroform as solvent.

Results and discussion

The use of standard and recently proposed ^1H - ^1H homodecoupling NMR schemes, in combination with DFT-GIAO-SCRF approach as an attractive method to propose valid 3D-structures of hydrocarbons by using lup-20(29)-ene PT as model is described. Full proton $\{^1\text{H}\}$ to carbon $\{^{13}\text{C}\}$ chemical shift assignments are done by even slight modifications of key parameters in standard schemes and by implementing NMR-pure shift technology, that has recently shown its potential for studies in complex systems with important signal overlap [14, 16]. Advantages of the use of this set of NMR schemes for signal assignment are evaluated by agreements with respect calculated ^1H and ^{13}C chemical shifts of lup-20(29)-ene ($\text{C}_{30}\text{H}_{50}$), in turn obtained by gauge invariant atomic orbitals-density functional theory approach, considering the effect of solvation in predicted NMR observables [33, 34].

Figure 1 (bottom) depicts a standard one-dimensional proton NMR spectrum ($1\text{D-}^1\text{H}$ NMR) of lup-20(29)-ene, whereas a set of 47 different CH_3 (21 protons), CH_2 (22 protons) and CH (4 protons) spin systems of the $\text{C}_{30}\text{H}_{50}$ moiety, present chemical shifts between 0.73 and 1.86 ppm. Such amount of homonuclear coupled

resonances defined in a narrow spectral width, evidently complicates a direct assignment from the $1\text{D-}^1\text{H}$ -spectrum. Severe signal overlap can be partially alleviated with an instant-homodecoupling real time pure shift $1\text{D-}^1\text{H}$ NMR scheme (Fig. 1, top). Collapse of short-to-long range scalar couplings ($^n\text{J}_{\text{H-H}}$) _{$n=3, 4, 5$} by homodecoupling, aids to partially resolve some of the ^1H lup-20(29)-ene resonances, like for instance the pure shift singlets appearing between 1.84 ppm (H15_1, H15_2); 1.697–1.592 ppm (H22_1, H11_1, H3_1); 1.59–1.51 ppm (H2_1, H6_1); 1.50–1.45 ppm (H7_1, H11_2, H12_1); 1.43–1.32 ppm (H1_1, H9, H12_2, H16_1, H18, H6_2, H2_2); 1.30–1.17 ppm (H21_1, H21_2, H1_2, H13, H7_2) and 1.16–0.7 ppm (H16_2, H3_2, H28, H26, H24, H25, H23, H22_2, H27 and H5). However, said assignment was confirmed by the pure shift method and previously done by the following NMR schemes.

Undoubtedly, ^1H chemical shift assignments of complex C_{30} triterpenes, limited by a poor chemical shift dispersion, have to be done by simultaneously assigning their attached ^{13}C spin systems, defined in a more dispersed frequency range [35]. For that, local chemical environments, hybridizations and type of carbons of lup-20(29)-ene, were characterized by stacking a

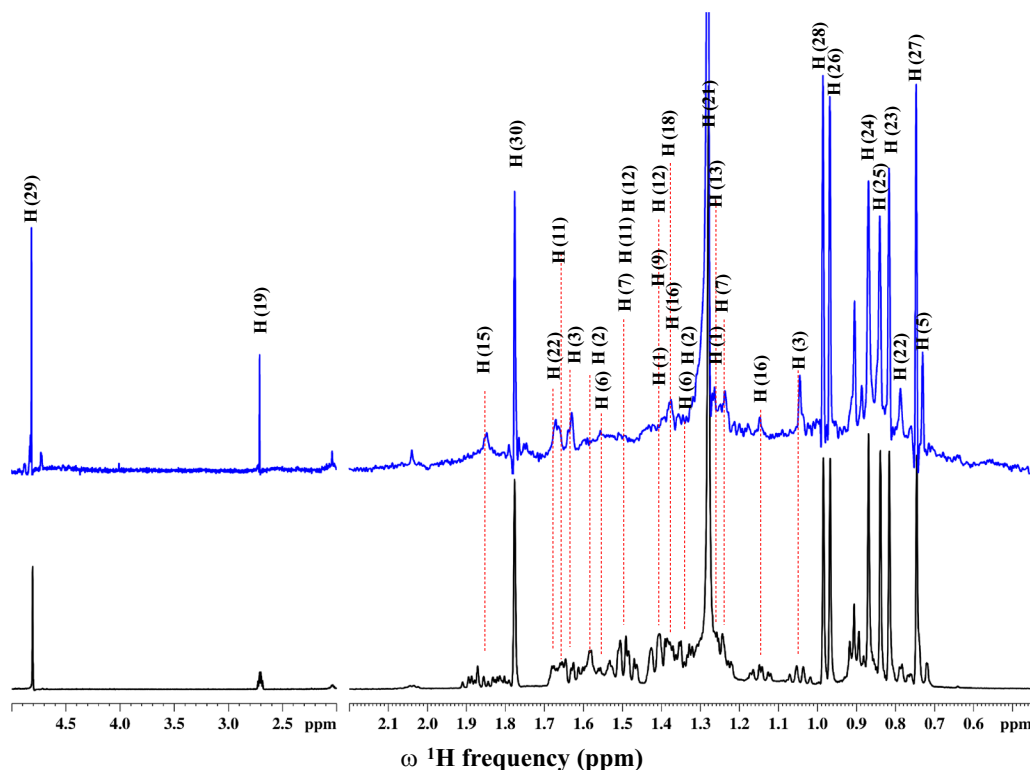


Fig. 1 Full assignment of lup-20(29)-ene ^1H NMR resonances depicted within the standard proton direct excitation spectrum (black, bottom) and the real-time ^1H broadband instant-homodecoupling Zangger-Sterk pure shift experiment (blue, top)

(See figure on next page.)

Fig. 2 Full assignment of lup-20(29)-ene ^{13}C NMR resonances shown within an overlay between a ^{13}C -direct excitation semi-quantitative experiment and a DEPT- ^{13}C spectrum, wherein the later was used to disentangle all lupene's carbon spin systems. Relative integration of all ^{13}C resonances was done with respect the vinylic CH_2 (29) resonance

semi-quantitative one-dimensional carbon-13 NMR spectrum (1D- ^{13}C NMR) with a Distortionless Enhancement by Polarization Transfer with a 135° pulse angle (DEPT-135) [36] 1D- ^{13}C NMR spectrum, schemed in Fig. 2, and Additional file 1: Figure S3.

Stacked 1D- ^{13}C NMR in Fig. 2 confirms chemical shift ranges of seven CH_3 (sp^3) eleven CH_2 with sp^3 hybridation, one CH_2 with sp^2 , five CH (sp^3), five C' (sp^3) and one vinylic C' . Deep inspection of both stacked 1D- ^{13}C plots confirms the presence of overlaid resonances in different ranges: 21.63–20.875 ppm [CH_2 (11), CH_3 (23), CH_2 (2)]; 33.586–33.215 ppm [CH_2 (1), CH_3 (24), CH_2 (7)] and 42.071–41.83 [CH_2 (16), C' (14), C' (8), C' (10), CH_2 (3)]. Once identified all types of carbons, even in severe overlap conditions, it becomes straightforward the full assignment of $^1\text{J}_{\text{C-H}}$ short range HSQC two-dimensional experiment (Additional file 1: Figure S4), particularly pointing out the easiness to discriminate non-trivial CH_2 resonances: CH_2 (6), CH_2 (2), CH_2 (11), CH_2 (12), CH_2 (15), CH_2 (7), CH_2 (1), CH_2 (22), CH_2 (3), CH_2 (16), respectively at $\delta^{13}\text{C} = 18.665, 20.875, 21.631, 23.995, 27.357, 33.215, 33.586, 40.276, 41.863$ and 42.071 ppm.

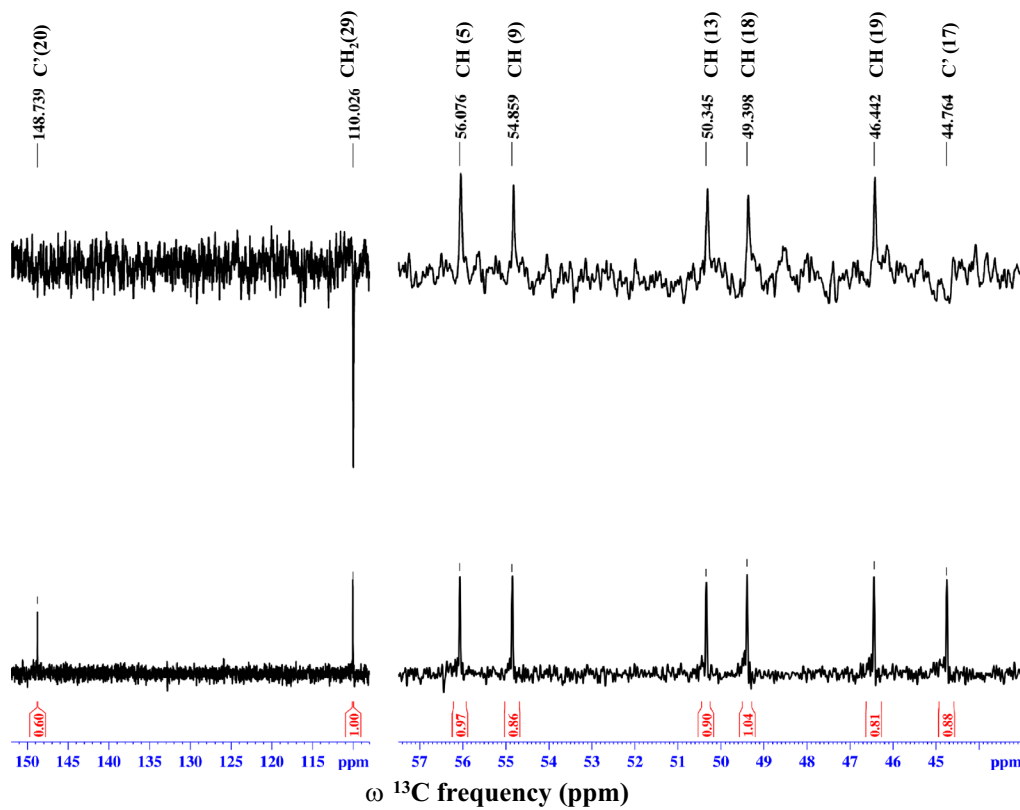
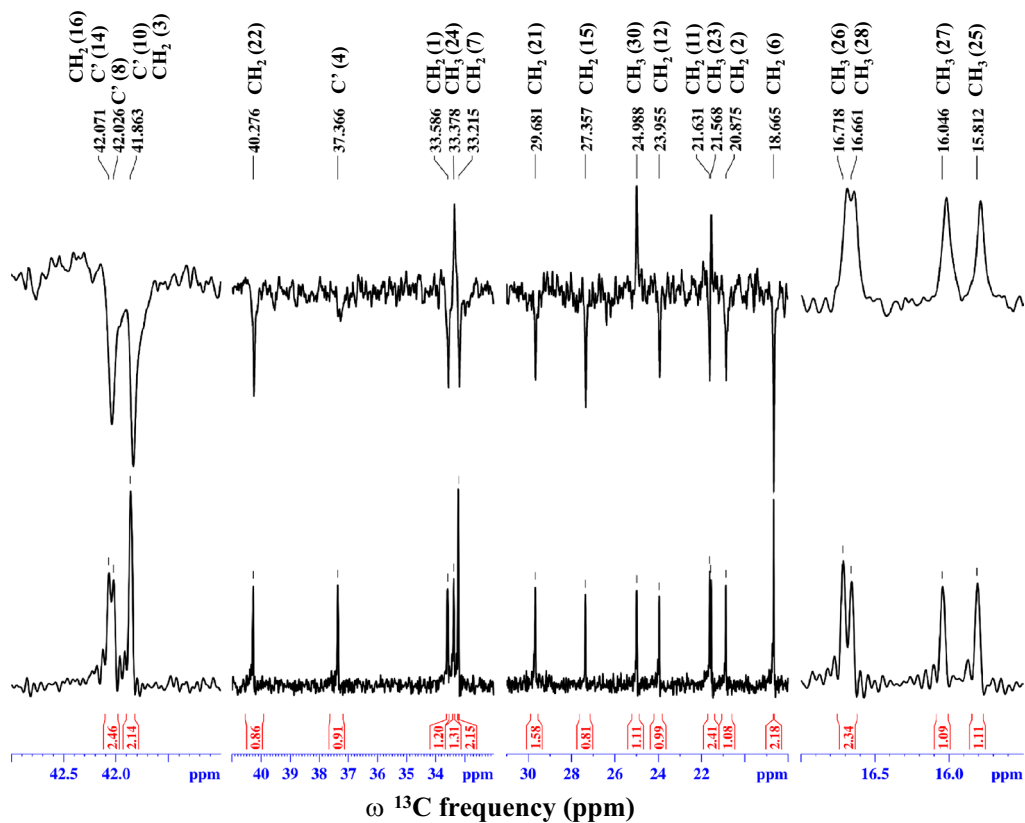
Next step comprises identification of seven methyl spin systems of lup-20(29)-ene. For instance, CH_3 (30) was unambiguously assigned by isolated HSQC correlations, respectively at $(\delta^{13}\text{C}, \delta^1\text{H}) = (24.988, 1.776)$ ppm, with the aid of its specific proton shift. An analog conception applies for CH_3 (24), which with a carbon-to-proton HSQC isolated correlation at 33.378, 0.8704 ppm, the specific carbon resonance of said moiety, allows an unambiguous assignment. CH_3 (23) presents as well an isolated carbon-to-proton HSQC correlation at 21.568, 0.818 ppm, with a carbon shift out of the range of 16.7–15.81 ppm, that allows its identification, despite its proton shift close to the rest of the methyl resonances. Interestingly, CH_3 (23) and CH_3 (24) carbon shifts are located in crowded CH_2 chemical shift regions, but identified with the aim of the DEPT-135 experiment (Fig. 2 and Additional file 1: Figure S3). In the other hand, identification of the rest of the methyl resonances [CH_3 (25), CH_3 (27), CH_3 (28), CH_3 (26)] comprises the use of additional NMR schemes.

The use of Heteronuclear Multiple Bond Coherence (HMBC) two-dimensional NMR experiment has shown its robustness for full assignment of terpenoids [13, 37], mostly in cases when functional groups like multiple bounds or heteroatoms within the hydrocarbon moiety

are present. For the present $\text{C}_{30}\text{H}_{50}$ case, the use of the HMBC technique at standard conditions for promoting short-to-long range $^n\text{J}_{\text{C-H}(n=3-5)}$ heteronuclear contacts [38], produces a spectrum with multiple overlays that difficult signal assignment, even for the isolated CH_3 (25), CH_3 (27), CH_3 (28), CH_3 (26) proton-to-carbon chemical shifts (Fig. 3, bottom). Thus, a proposed strategy to unambiguously assign methyls and their short-to-long range spin neighbors of lup-20(29)-ene, is to modify the long-range evolution period delay (d6, Additional file 1: Figure S5) associated to promote carbon-to-proton correlation contacts different from the $^1\text{J}_{\text{CH}}$ value [38], located just after the 90° hard pulse in ^1H channel in such a way to only promote the appearance of weak $^n\text{J}_{\text{CH}}$ heteronuclear contacts of around 2 Hz (Fig. 3, top). By increasing d6 from 62.5 ms (standard version, Fig. 3 bottom) to 250 ms (Fig. 3, top) it becomes straightforward to assign the following correlations: [H27– C' (8), C' (17), CH (18) and CH (9)]; [H23– CH_2 (7), CH_2 (3), CH (5)]; [H25– C' (4), CH (13), CH (5)]; [H(24)– CH_2 (7), CH_2 (3), CH (5)]; [H(26)– CH_2 (1), C' (8), CH (18)]; [H28– CH_2 (16), C' (14), CH (13)] and [H30–CH (19)] that served to discriminate all seven methyl spin systems within lup-20(29)-ene. A similar strategy was done for proton–proton through space assignments of lup-20(29)-ene with exchange spectroscopy spectra (EXSY, Fig. 4). As known, EXSY diagonal-to crosspeak buildup curves as a function of mixing time to retrieve internuclear distances [34] show minimum signal intensity values at longer mixing times. In consequence, EXSY experiments carried out at long mixing times, will produce two-dimensional experiments with cross-peaks of roughly weak dipolar H–H interactions, such as contacts involving methyls.

Figure 4 presents the proton–proton through-space EXSY experiment of lup-20(29)-ene with a mixing time of 1.4 s. Full set of retrieved correlations are schematized within the spatial representation of lup-20(29)-ene at the top of the figure. With said experimental conditions, through space correlations of methyl spin systems have been fully characterized, such as previously done with the HMBC experiment, optimized for weak through bond heteronuclear correlations.

Assignment strategy concludes with the use of a short-to-long range through bond homonuclear proton–proton scheme: Total Correlation Spectroscopy (TOCSY). As continuously highlighted within the present communication, the use of standard schemes to assign terpenes with



(See figure on next page.)

Fig. 3 Two-dimensional ^1H - ^{13}C HMBC correlation spectra of lup-20(29)-ene promoting; top: long range heteronuclear coupling contacts of around 2 Hz ($d_6 = 250$ ms) and bottom: promotion of $^{3,4,5}J_{\text{H-X}}$ short-to long range heteronuclear contacts of around 7 Hz ($d_6 = 62.5$ ms as the standard condition)

lack of multiple bonds and/or heteroatoms, produces spectra with severe signal overlap. TOCSY standard spectrum of the $\text{C}_{30}\text{H}_{50}$ lup-20(29)-ene (500 ms of mixing time) is depicted in Fig. 5, bottom. Assignment complications with the use of said conditions are self-explained within the figure. To alleviate said complications, the use of broadband proton homodecoupling using a Psyche element in F1 to produce a TOCSY pure shift experiment is proposed (Fig. 5, top).

To the best of our knowledge, Fig. 5 presents for the first time the advantages of using a two-dimensional TOCSY pure shift NMR experiment in PTs composed by only a hydrocarbon core. 2D-TOCSY pure shift not only allows a straightforward confirmation of short-to-long range through bond correlations of isolated spin systems like methyls, but mostly allows a broad assignment of spin correlations located close to the auto-correlation diagonal. Full setup of 2D-TOCSY broadband homodecoupling with a Psyche module comprises a further spectra symmetrization in order to produce pure shift signals in the direct F2 dimension.

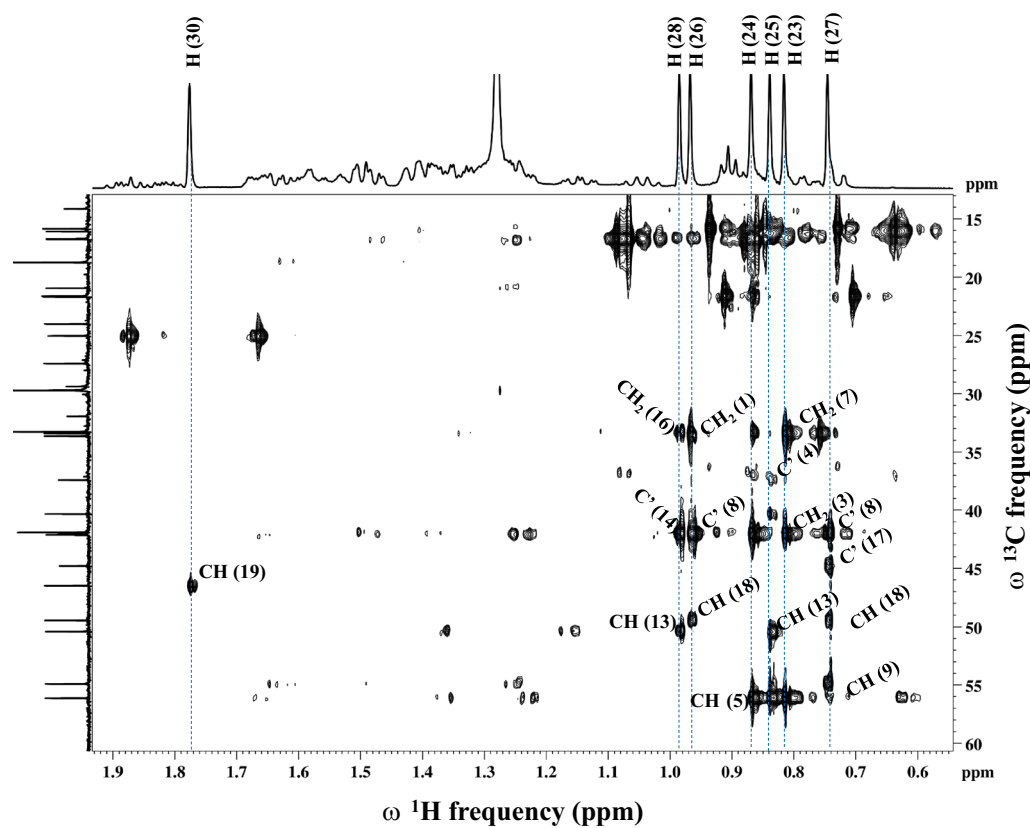
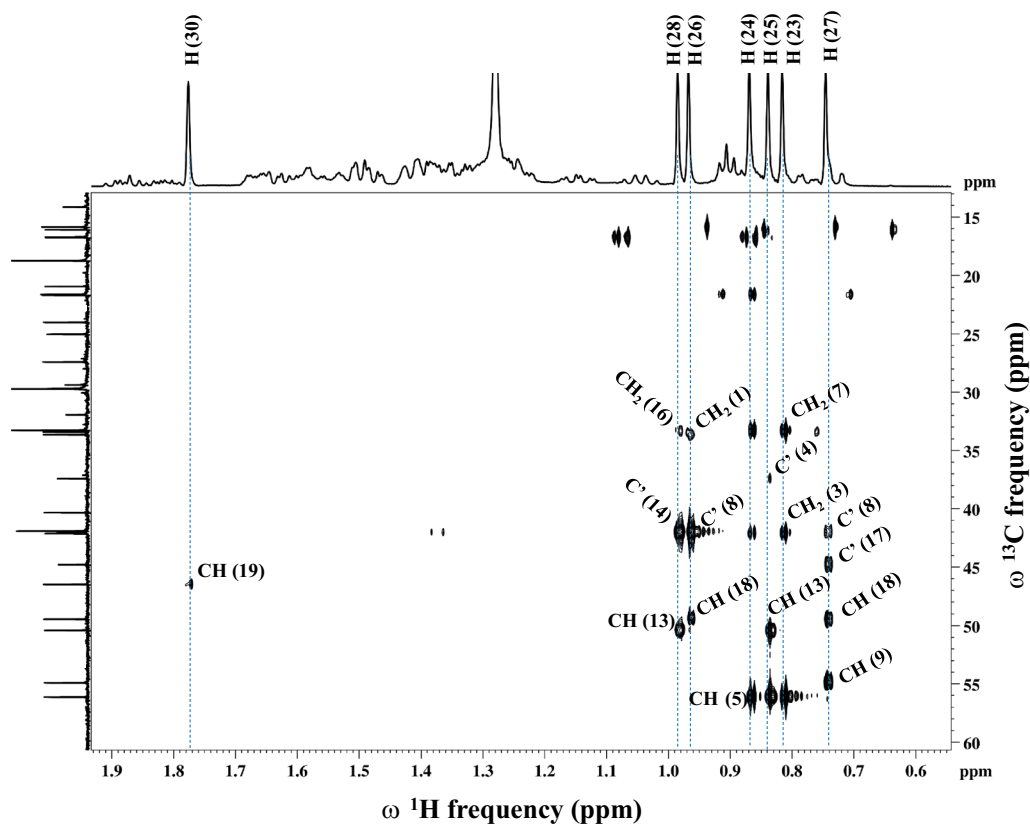
Once confirmed full assignment of $\text{C}_{30}\text{H}_{50}$ lup-20(29)-ene's chemical shifts with the combination of 1D- ^{13}C (DEPT), 2D- $\{^1\text{H}-^{13}\text{C}\}$ HMBC ($d_6 = 250$ ms), 2D- $\{^1\text{H}-^1\text{H}\}$ EXSY ($\tau_{\text{mix}} = 1400$ ms), 2D- $\{^1\text{H}-^1\text{H}\}$ TOCSY-pure shift ($\tau_{\text{mix}} = 500$ ms) and 1D- ^1H instant homodecoupling pure shift, validation of the full set of assigned proton-to-carbon chemical shifts was carried out by comparing agreements between experimental NMR data and calculated shifts of an optimized electronic structure by means of the DFT-GIAO approach.

Additional file 1: Figure S6 presents the three-dimensional atomic coordinates of lup-20(29)-ene, whereas optimized electronic structure of the present PT was obtained by considering the effects of chloroform implicit solvation, likewise the used solvent in the NMR experiments.

The single point DFT-GIAO calculation of chemical shift tensors from a stable local minimum, derived in turn into theoretical isotropic shifts, compared with the experimental data are shown in Fig. 6. Excellent agreements were found for the full set of experimental-predicted thirty carbon chemical shifts ($R^2 = 0.9842$) of lup-20(29)-ene. In a lesser extent, it is reported as well the experimental-theoretical proton chemical shift agreements ($R^2 = 0.9283$), whereas disagreements are most probably due to known challenges to predict the

full set of contributions that describe methylenes' proton local chemical environments, with DFT-GIAO approaches [39].

As conclusion, this work presents a strategy for a full unambiguous NMR chemical shift assignment of a key triterpene precursor of important metabolites in plants: the hydrocarbon PT $\text{C}_{30}\text{H}_{50}$ lup-20(29)-ene. Its chemical nature imposes restrictions for structural studies, for instance standard NMR or X-Ray diffraction spectroscopy. For that, it is proposed a set of standard and recently proposed NMR schemes at specific acquisition conditions, combined with robust quantum chemistry calculations to propose a 3D-structure of lup-20(29)-ene, in agreement with experimental observables. Said strategy allows to disentangle keen differences in severe signal overlap situations of similar type of hydrocarbons: carbon hybridization, proton diasterotopic effects and long-range through-bond or through-space vicinities of identified spin systems. To the best of our knowledge this work presents for the first time the advantages of using pure shift proton homodecoupling schemes for PTs. Correlations between experimental and theoretical NMR chemical shifts strongly suggest the agreement of the 3D-carbon skeleton of lup-20(29)-ene herein proposed. Limitations of the proposed assignment workflow for full assignment of PTs is in terms of NMR sensitivity as a function of sample concentration. For the present study, approximately 30 mg of lup-20(29)-ene were dissolved in 0.5 mL of CDCl_3 . As a reference, said concentration allowed to have ^1H and ^{13}C direct detection NMR experimental times of respectively 6' 51" and 11 h 12' 6". For heteronuclear transfer experiments, sensitivity enhancement with respect ^{13}C direct detection experiments, allowed to acquired DEPT (signal to noise enhancement factor of 4 respect ^{13}C direct detection), HSQC and HMBC (signal to noise enhancement factor of 32 respect ^{13}C direct detection in both cases) in reasonable experimental times [38]. Finally, Zangger-Sterk broadband homodecoupling pure shift schemes present a typical sensitivity of 0.5–2.0% with respect an arbitrary 100% sensitivity of a ^1H direct detection experiment [23, 25], producing in our case an experimental time of 3 h 10' 56" in order to have comparable signal to noise ratios (Fig. 1). For that, the present method would produce forbidden NMR experimental times for both heteronuclear



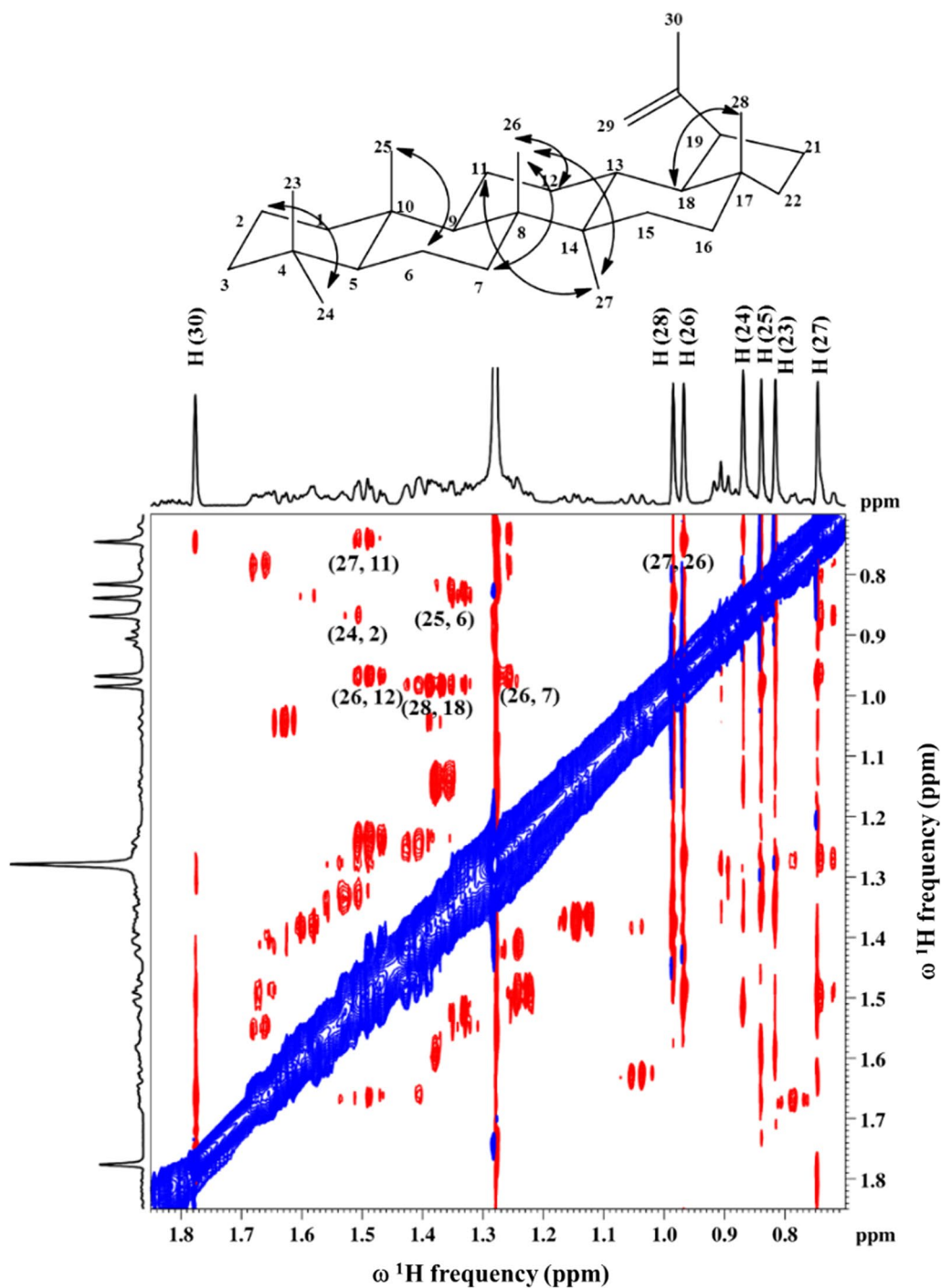
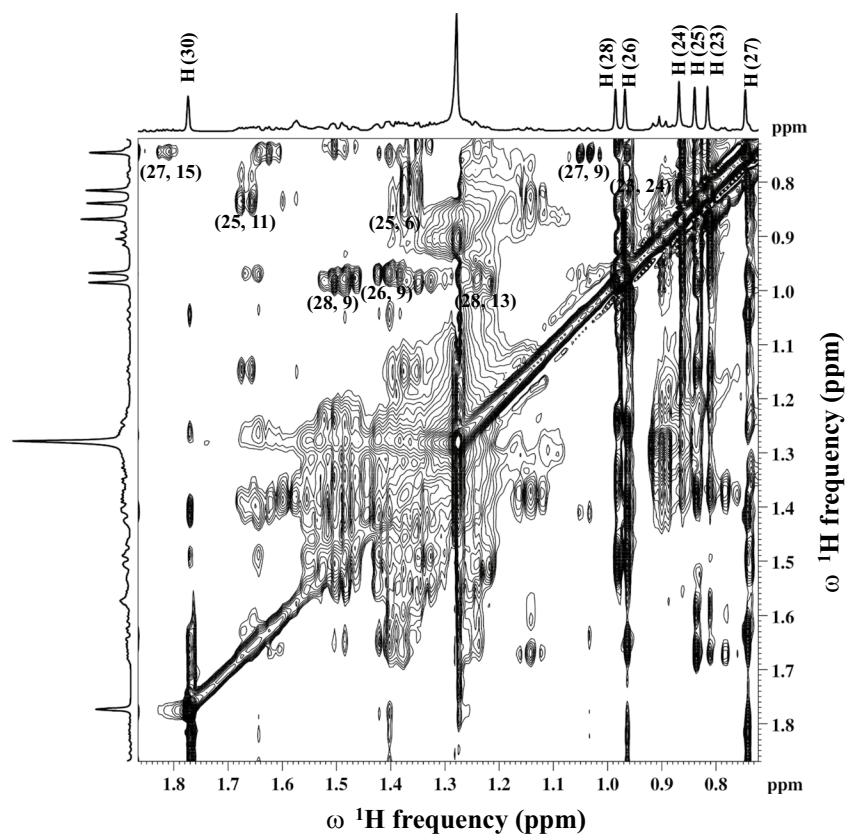
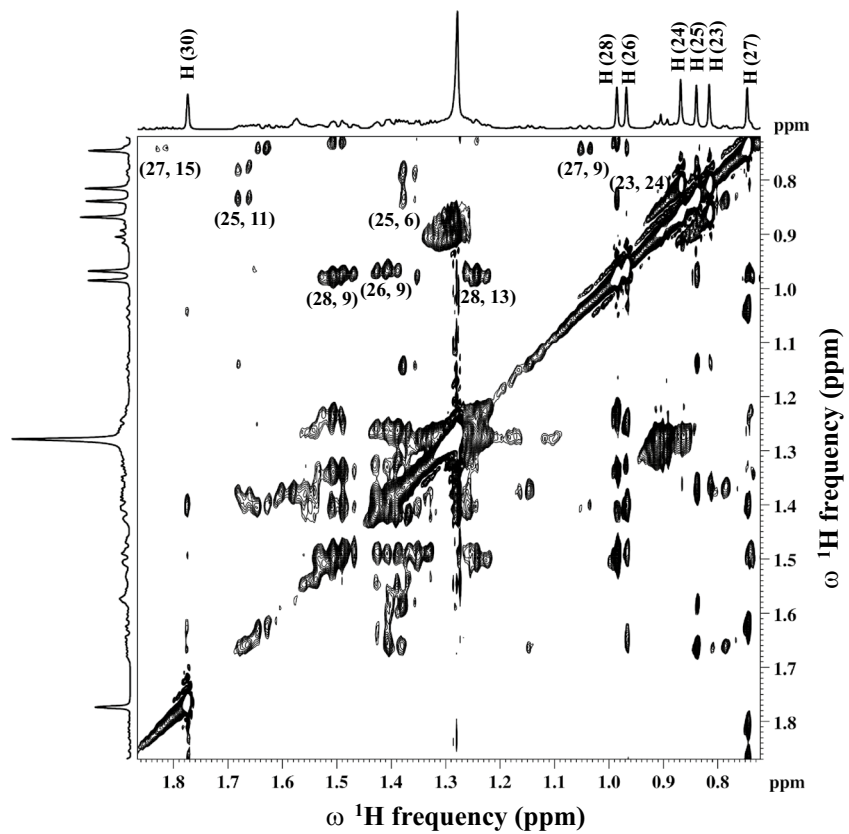
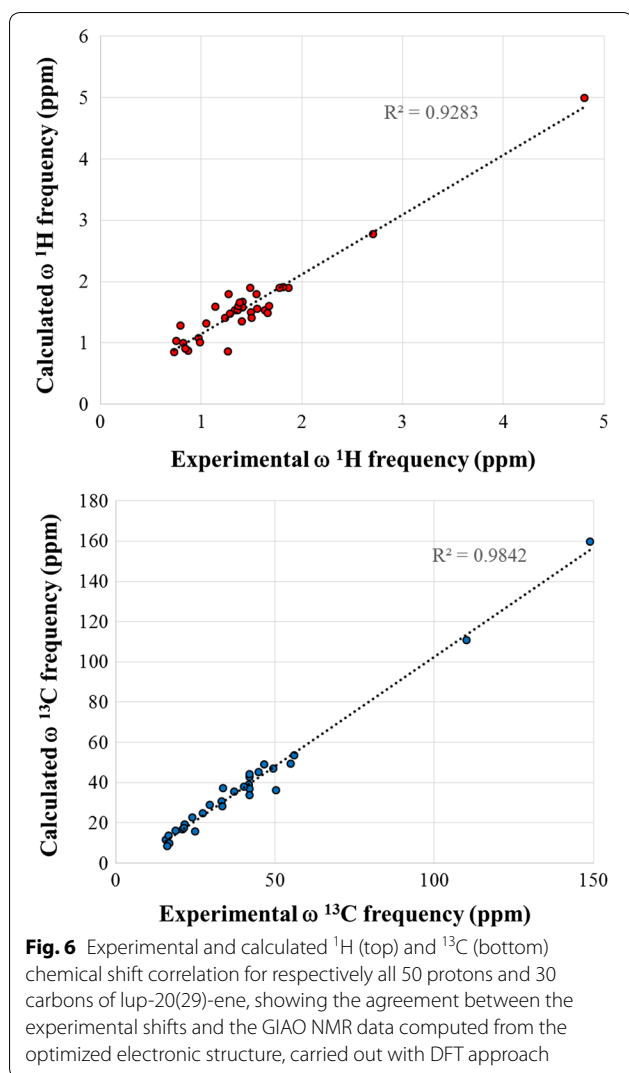


Fig. 4 Two-dimensional ^1H - ^1H homonuclear correlation spectrum via dipolar coupling (EXSY) of lup-20(29)-ene, with 1.4 s of mixing time. Key inter-nuclear correlations between resonances involving methyls are shown in the spectrum, as well as in the molecular formula

(See figure on next page.)

Fig. 5 Two-dimensional TOCSY proton-proton homonuclear correlation spectra, using a Hartman-Hahn transfer with a DIPSI element, promoting ^1H - ^1H long range through bound contacts with 500 ms of mixing time. Top: Broadband proton homodecoupling using Psyche element in F1 and further spectral symmetrization. Bottom: Standard scheme with no pure shift Proton homodecoupling





transfer and pure shift methods for diluted samples with below or close to 10 mg of available PTs.

Additional file

Additional file 1. Electronic impact and high-resolution Electrospray ionization mass spectrometry characterization, full chemical shift window of 1D- ^{13}C (DEPT), HMBC modified parameter schemed within the pulse sequence, optimized 3D-electronic structure of lup-20(29)-ene and NMR workflow for full assignment of a $\text{C}_{30}\text{H}_{50}$ PT, with chemical shift and structural cross-check validation with the DFT-GIAO approach are described.

Acknowledgements

Authors acknowledge the Mexican Ministry of Science and Technology (CONACyT) for funding: CONACyT program No. 682 "Cátedras Conacyt", CONACyT program No. LN295321 "Laboratorios Nacionales" (J.E.H-P) and CONACyT-Mexico Grant INFRA-2016 (269012) for funding Nuclear Magnetic Resonance experimental time. Authors acknowledged the Dirección General de

Cómputo y de Tecnologías de Información y de Comunicación (DG TIC) at Universidad Nacional Autónoma de México, Project: LANCAD-UNAM-DGTIC-154 that allowed computational time for GIAO-DFT-SCRF calculations. C.M.-J. is a CONACyT 431073 scholarship holder.

Authors' contributions

JEH-P: Conceptualization, NMR resources, methodology, investigation, formal analysis, writing-review and editing. CM-L: Collection and identification of plant material, investigation. BR-T: Investigation, review. LR: Software, investigation. H.Z-P: Resources, supervision, funding acquisition, investigation, writing-original draft, review. All authors read and approved the final manuscript.

Competing interests

The authors declare that they have no competing interests.

Author details

¹ Consejo Nacional de Ciencia y Tecnología – Laboratorio Nacional de Investigación y Servicio Agroalimentario y Forestal, Universidad Autónoma Chapingo, Km. 38.5 Carretera México-Tezcoco, 56230 Chapingo, Estado de México, Mexico. ² Laboratorio de Productos Naturales, Área de Química, Departamento de Preparación Agrícola, AP 74 Oficina de Correos Chapingo, Universidad Autónoma Chapingo, Km. 38.5 Carretera México-Tezcoco, 56230 Chapingo, Estado de México, Mexico. ³ Departamento de Química Orgánica, Facultad de Química, Universidad Nacional Autónoma de México, Ciudad Universitaria, Delegación Coyoacán, 04510 Mexico City, Mexico.

Received: 18 February 2019 Accepted: 3 May 2019

Published online: 11 May 2019

References

- Hill RA, Connolly JD (2018) Triterpenoids. *Nat Prod Rep*. <https://doi.org/10.1039/C8NP00029H>
- Hill RA, Connolly JD (2017) Triterpenoids. *Nat Prod Rep* 34:90–122
- Hill RA, Connolly JD (2015) Triterpenoids. *Nat Prod Rep* 32:273–327
- Hill RA, Connolly JD (2013) Triterpenoids. *Nat Prod Rep* 30:1028–1065
- Hill RA, Connolly JD (2012) Triterpenoids. *Nat Prod Rep* 29:780–818
- Xu R, Fazio GC, Matsuda SP (2004) On the origins of triterpenoid skeletal diversity. *Phytochemistry* 65:261–291
- Dzubak P, Hajduch M, Vydra D, Hustova A, Kvasnica M, Biedermann D, Markova L, Urban M, Sarek J (2006) Pharmacological activities of natural triterpenoids and their therapeutic implications. *Nat Prod Rep* 23:394–411
- Sheng H, Sun H (2011) Synthesis, biology and clinical significance of pentacyclic triterpenes: a multi-target approach to prevention and treatment of metabolic and vascular diseases. *Nat Prod Rep* 28:543–593
- Laszczyk MN (2009) Pentacyclic triterpenes of the lupine, oleanane and ursane group as tools in cancer therapy. *Planta Med* 75:1549–1560
- Sharma H, Kumar P, Deshmukh RR, Bishayee A, Kumar S (2018) Pentacyclic triterpenes: new tools to fight metabolic syndrome. *Phytomedicine* 50:166–177
- Kuo R-Y, Qian K, Morris-Natschke SL, Lee K-H (2009) Plant-derived triterpenoids and analogues as antitumor and anti-HIV agents. *Nat Prod Rep* 26:1321–1344
- Alqahtani A, Hamid K, Kam A, Wong K, Abdelhak Z, Razmovski-Naumovski V, Chan K, Li K, Groundwater P, Li G (2013) The pentacyclic triterpenoids in herbal medicines and their pharmacological activities in diabetes and diabetic complications. *Curr Med Chem* 20:908–931
- Breton RC, Reynolds WF (2013) Using NMR to identify and characterize natural products. *Nat Prod Rep* 30:501–524
- Jäger S, Trojan H, Kopp T, Laszczyk MN, Scheffler A, Jäger S, Trojan H, Kopp T, Laszczyk M, Scheffler A (2009) Pentacyclic triterpene distribution in various plants—rich sources for a new group of multi-potent plant extracts. *Molecules* 14:2016–2031
- Zhou J, Li C-J, Yang J-Z, Ma J, Li Y, Bao X-Q, Chen X-G, Zhang D, Zhang D-M (2014) Lupane triterpenoids from the stems of *Euonymus carnosus*. *J Nat Prod* 77:276–284

16. Rychnovsky SD (2006) Predicting NMR spectra by computational methods: structure revision of hexacyclinol. *Org Lett* 8:2895–2898
17. Kutateladze AG, Reddy DS (2017) High-throughput in silico structure validation and revision of halogenated natural products is enabled by parametric corrections to DFT-computed ¹³C NMR chemical shifts and spin–spin coupling constants. *J Org Chem* 82:3368–3381
18. Asakawa Y, Ludwiczuk A (2017) Chemical constituents of bryophytes: structures and biological activity. *J Nat Prod* 81:641–660
19. Delgadillo-Moya C (2014) Biodiversidad de *Bryophyta* (musgos) en México. *Revista Mexicana de Biodiversidad* 85:100–105
20. Brinkmeier E, Geiger H, Zinsmeister HD (2000) The cooccurrence of different biflavonoid types in *Pilotrichella flexilis*. *Z Naturforsch C* 55:866–869
21. Méjanelle L, Rivière B, Pinturier L, Khripounoff A, Baudin F, Dachs J (2017) Aliphatic hydrocarbons and triterpenes of the Congo deep-sea fan. *Deep Sea Res Part II* 142:109–124
22. Dujie H, Linye Z, Tieguan W (2010) Distribution patterns of pentacyclic triterpenoid hydrocarbons in low-mature source rocks from Eastern China. *Acta Geol Sin En Ed* 72:399–408
23. Herbert-Pucheta JE, Pitoux D, Grison CM, Robin S, Merlet D, Aitken DJ, Giraud N, Farjon J (2015) Pushing the limits of signal resolution to make coupling measurement easier. *Chem Commun* 51:7939–7942
24. Braunschweiler L, Ernst R (1983) Coherence transfer by isotropic mixing: application to proton correlation spectroscopy. *J Magn Reson* 53:521–528
25. Foroozandeh M, Adams RW, Nilsson M, Morris GA (2014) Ultrahigh-resolution total correlation NMR spectroscopy. *J Am Chem Soc* 136:11867–11869
26. Ammann W, Richarz R, Wirthlin T, Wendisch D (1982) ¹H and ¹³C chemical shifts and coupling constants of lupane application of two-dimensional NMR techniques. *Org Magn Reson* 20:260–265
27. Frisch MJ, Trucks GW, Schlegel HB, Scuseria GE, Robb MA, Cheeseman JR, Scalmani G, Barone V, Mennucci B, Petersson GA, Nakatsuji H, Caricato M, Li X, Hratchian HP, Izmaylov AF, Bloino J, Zheng G, Sonnenberg JL, Hada M, Ehara M, Toyota K, Fukuda R, Hasegawa J, Ishida M, Nakajima T, Honda Y, Kitao O, Nakai H, Vreven T, Montgomery JA Jr, Peralta JE, Ogliaro F, Bearpark M, Heyd JJ, Brothers E, Kudin KN, Staroverov VN, Kobayashi R, Normand J, Raghavachari K, Rendell A, Burant JC, Iyengar SS, Tomasi J, Cossi M, Rega N, Millam JM, Klene M, Knox JE, Cross JB, Bakken V, Adamo C, Jaramillo J, Gomperts R, Stratmann RE, Yazyev O, Austin AJ, Cammi R, Pomelli C, Ochterski JW, Martin RL, Morokuma K, Zakrzewski VG, Voth GA, Salvador P, Dannenberg JJ, Dapprich S, Daniels AD, Farkas Ö, Foresman JB, Ortiz JV, Cioslowski J, Fox DJ (2009) Gaussian 09, Revision D.01. Gaussian Inc., Wallingford, CT
28. Iqbal Choudhary M, Ali S, Anjum S (2006) 1,13-Dimethyl-6H,7H,8H-chromeno[3',4':5,6]pyrano[3,2-c]chromene-6,8-dione. *Acta Cryst E* 62:o1352–o1354
29. Becke AD (1993) Density-functional thermochemistry III. The role of exact exchange. *J Chem Phys* 98:5648–5652
30. Lee CT, Yang WT, Parr RG (1988) Development of the Colle–Salvetti correlation-energy formula into a functional of the electron density. *Phys Rev B* 37:785–789
31. Helgaker T, Watson M, Handy NC (2000) Analytical calculation of nuclear magnetic resonance indirect spin-spin coupling constants at the generalized gradient approximation and hybrid levels of density-functional theory. *J Chem Phys* 113:9402–9409
32. Tomasi J, Cammi R, Mennucci B, Cappelli C, Corni S (2002) Molecular properties in solution described with a continuum solvation model. *Phys Chem Chem Phys* 4:5697–5712
33. Herbert-Pucheta JE, Candy M, Colin O, Requet A, Bourdreux F, Galmiche-Loire E, Gaucher A, Tomassigny C, Prim D, Mahfoudh M, Leclerc E, Campagne J-M, Farjon J (2015) Understand, elucidate and rationalize the coordination mode of pyrimidylmethylamines: an intertwined study combining NMR and DFT methods. *Phys Chem Chem Phys* 17:8740–8749
34. Herbert-Pucheta JE, Prim D, Gillet J-M, Farjon J (2016) Deciphering the conformational choreography of zinc coordination complexes with standard and novel proton NMR techniques combined with DFT methods. *Chem Phys Chem* 17:1–13
35. Mahato SB, Kundu AP (1994) ¹³C NMR spectra of pentacyclic triterpenoids—a compilation and some salient features. *Phytochemistry* 37:1517–1574
36. Primasova H, Bigler P, Furrer J (2017) The DEPT experiment and some of its useful variants. *Annu Rep NMR Spectrosc* 92:1–82
37. Lai Y-C, Chen C-K, Tsai S-F, Lee S-S (2012) Triterpenes as α-glucosidase inhibitors from *Fagus hayatae*. *Phytochemistry* 74:206–211
38. Furrer JA (2012) Comprehensive discussion of HMBC pulse sequence part 1: the classical HMBC. *Concepts Magn Reson A* 40:101–127
39. Borowski P (2012) Conformational analysis of the chemical shifts for molecules containing diastereotopic methylene protons. *J Magn Reson* 214:1–9

Publisher's Note

Springer Nature remains neutral with regard to jurisdictional claims in published maps and institutional affiliations.